Atmospheric Research 197 (2017) 94–104

Contents lists available at ScienceDirect

Atmospheric Research

journal homepage: www.elsevier.com/locate/atmosres

Spatiotemporal variations and regional differences of extreme precipitation events in the Coastal area of China from 1961 to 2014

Xiaoli Wang[a,b,c], Xiyong Hou[a,c,*], Yuandong Wang[d]

[a] Yantai Institute of Coastal Zone Research, Chinese Academy of Sciences, Yantai 264003, China
[b] University of Chinese Academy of Sciences, Beijing 100049, China
[c] Key Laboratory of Coastal Environmental Processes and Ecological Remediation, Key Laboratory of Coastal Environmental Processes and Ecological Remediation, Chinese Academy of Sciences, Yantai 264003, China
[d] Gannan Normal University, Ganzhou 341000, China

ARTICLE INFO

Keywords:
Extreme precipitation events
Spatial-temporal variation
Regional difference
Coastal area of China

ABSTRACT

Coastal area of China (CAC) is of high ecological vulnerability and extremely sensitive to global climate change. Based on daily precipitation dataset of 156 station records, spatial and temporal variations of extreme precipitation events from 1961 to 2014 in the coastal area of China were investigated using a set of mathematical and statistical methods including trend analysis, R/S analysis, wavelet analysis, Mann-Kendall test, accumulative anomaly analysis and Pettitt test. Results revealed that there was a generally insignificant upward and downward tendency of extreme precipitation events in the southern and northern coastal area, respectively. Persistent of tendency suggested that trends of extreme precipitation events in Huabei, Huanghuai, Jiangnan and Huanan coastal areas would continue but trends in Dongbei and Jianghuai coastal areas would mostly present contrary to the past in the future. Multi-year averages of all extreme precipitation indices except consecutive dry days (CDD) varied largely in the coastal area of China, generally highest in Huanan coastal area and lowest in Huabei coastal area. The primary period of extreme precipitation indices varied from 2- to 7-year in the sub-regions. The abrupt change of extreme precipitation indices occurred mainly in the 1990s and the 1970s in the CAC.

1. Introduction

As important indicators for measuring precipitation intensity and frequency increase or not, extreme precipitation events are sensitive in reflecting climate change (Knapp et al., 2008). With global warming, the surface evapotranspiration is increasing and the water cycle is accelerating, which leads to extreme precipitation events occurring frequently in many countries and regions around the world (Zhang et al., 2009; Cavalcanti, 2012; Madsen et al., 2014), thus bringing numerous negative effects worldwide. On the one hand, frequent occurrence of extreme precipitation events increases the randomness of water supply, and limits the water resources allocation and scheduling, which result in gradual reduction of available water resources (Subash et al., 2011; Cavalcanti et al., 2015). On the other hand, extreme precipitation events with increasing frequency induce the secondary disasters and derivative disasters, such as floods, droughts, landslides, debris flow, and so on, which pose a huge challenge and a serious threat for socio-economic sustainable development, natural environment and eco-system as well as people's properties and lives (Li et al., 2011; Jiang et al., 2015; Powell and Reinhard, 2016). Consequently, extreme precipitation events have received widespread concern due to their large-scale and negative impacts.

Temporal and spatial characteristics of extreme precipitation events at global, continental, national and regional scales have been studied and reported. In a global perspective, a significant upward trend of rain days was found throughout the 20th century (Alexander et al., 2006). Over global land, the frequency of light precipitation events decreased over East China and northern Eurasia but increased over United States, Australia and the Iberian Peninsula, however, the intensity trends are opposite to those in frequency from 1961 to 2010 (Wen et al., 2015). On continental scale, extreme precipitation indices presented upward trends in North America during the 20th century (Griffiths and Bradley, 2007). Significant regional differences were detected in extreme precipitation events in South America, which had been associated with large scale events such as El Niño-Southern Oscillation, Atlantic SST, atmospheric circulation, and so on (Cavalcanti, 2012). Studies on extreme precipitation events in Europe demonstrated that the precipitation extremes increased on the whole in recent years (Päädam and Post, 2011; Rimkus et al., 2011; Boccolari and Malmusi, 2013; Croitoru et al., 2013; Willems, 2013), and this increase would continue in the future

* Corresponding author at: Yantai Institute of Coastal Zone Research, Chinese Academy of Sciences, Yantai 264003, China.
E-mail address: xyhou@yic.ac.cn (X. Hou).

http://dx.doi.org/10.1016/j.atmosres.2017.06.022
Received 6 January 2017; Received in revised form 13 June 2017; Accepted 20 June 2017
Available online 21 June 2017
0169-8095/

(Madsen et al., 2014). In parts of Africa, extreme precipitation events have been mutated from a low-frequency period into a high-frequency period (Tramblay et al., 2012; Ly et al., 2013). In Asia, Cinco et al. (2014) investigated the variation of extreme precipitation events based on the daily precipitation data of gauge stations and found that there were significant upward trends about the frequency and intensity for extreme daily precipitation events in Philippines from 1951 to 2010. During the past 30 years, a decrease of precipitation had occurred in the whole Indian (Naidu et al., 2015), but an increase of extreme precipitation events at regional scale had been observed (Subash et al., 2011; Jena et al., 2014). The extreme precipitation indices showed an upward trend in Georgia during 1971–2010, and some extreme precipitation events such as heavy rain days' contribution to annual total precipitation amount was increasing (Keggenhoff et al., 2014).

In China, extreme precipitation events generally increase but present significant spatial differences with larger amplitudes in the western and southern region while smaller in the northern region (Xu et al., 2011; You et al., 2011). On the regional scale, characteristics of extreme precipitation events are more diversified in China. For instance, the annual total precipitation amount decreased slightly, but the frequency and intensity in extreme precipitation and concentration of precipitation both increased in Southwest of China since the 1950s (Ding, 2014). Some studies documented that extreme precipitation varied largely in the Northwest semi-arid region of China, with a higher upward trend in the north than that in the south, and some extreme precipitation indices such as Very wet day, Number of precipitation days and Daily intensity index showed much greater (stronger) variations in mountain areas than in plains due to the impacts of terrain (Zhang et al., 2011; Wang et al., 2013; Deng et al., 2014). In the south of China, a remarkable spatial pattern in extreme precipitation was detected, i.e., the closer to the northwest the dryer, while the closer to the southeast the wetter (Ren et al., 2014). In addition, it is also found that extreme precipitation events showed significant regional differences at the scale of provincial and watershed in China (Nie et al., 2012; Zhao et al., 2014; Chen et al., 2015; Song et al., 2015).

The Coastal Area of China (CAC) is the transitional zone between Eurasia and the western Pacific Ocean, and the natural environmental of this area is very complex and easily changeable because of the large-scale and frequent material transfer and energy flux exchange between land and ocean system (Yi et al., 2011). With large population density, intensive industries and facilities, and rapid economic development, the CAC is highly vulnerable to various disasters such as typhoons, storm surge, coastal erosion, seawater intrusion and wetland degradation. Furthermore, with global climate change, extreme climate events, for example, heat waves, freezing events, heavy precipitation events and droughts occur frequently, which lead to the deterioration of regional ecological environment and the increase of vulnerability over CAC (Dong et al., 2010; Jiao et al., 2015).

Recently, spatial and temporal variations in extreme precipitation events have been documented in several studies about the CAC. For instance, Wang et al. (2014) investigated drought and flood characteristics in southeast coast and found that the drought showed a pattern of "south-less and north-more", and on the contrary, flood is characterized by a pattern of "south-heavy and north-light". Jiang et al. (2011) assessed the extreme precipitation trend over Circum-Bohai-Sea region and found that the precipitation extremes showed declining trends and significant decadal variations.

However, as a transitional zone linking the ocean and inland, few studies have regard to characteristics of extreme precipitation events in the CAC as a whole. Furthermore, considering the large span of latitude from north to south, huge complexity and diversity of climate, topography and underlying surface conditions, it is necessary to make a comprehensive analysis of the variations of extreme precipitation events by combining the geographical features and climate types of the CAC. In this study, the spatial and temporal variations of extreme precipitation events in the CAC from 1961 to 2014 are examined in order to identify and quantify characteristics and regularities of extreme precipitation events, and provide reference and basis for scientific adaptation, mitigation and response to climate anomalies in the coastal area. Specifically, aims of this study are as follows: (1) to derive extreme precipitation indices based on the daily precipitation data of surface meteorological stations; (2) to reveal spatial patters of extreme precipitation events; (3) to explore temporal characteristics of extreme precipitation events from the perspective of tendency, persistence of tendency, periodicity and abruptness in the CAC.

The outline of this paper is as follows: Section 2 describes the study area, dataset and methods used to evaluate extreme precipitation events; Section 3 presents the results of observed spatial and temporal variability of extreme precipitation events, finally, discussion and conclusion are presented in Section 4.

2. Data and methods

2.1. Study area

According to the division boundary of Chinese provincial administrative, the region with spatial domain covering coastal provinces are identified as the study area (except Taiwan, the South China Sea islands and waters), hereinafter referred to as Coastal Area of China (CAC) in this study. In order to highlight the regional difference of extreme precipitation events, the CAC is divided into six sub-regions based on the China Meteorological and Geographical Regionalization put forward by the China Meteorological Administration. The sub-regions are renamed as coastal area of Dongbei (I), Huabei (II), Huanghuai (III), Jianghuai (IV), Jiangnan (V) and Huanan (VI) respectively from north to south (Fig. 1). Climatically, the northern part of the CAC, i.e., regions I, II and III belong to the temperate zone and warm temperate zone, and the southern part, i.e., regions IV, V and VI pertain to the subtropical zone and tropical zone. The annual mean temperature is increasing gradually from 8.6 °C in region I to 21.5 °C in region VI. The annual total precipitation in the southern CAC is higher than that in the northern, with the minimum in region II of 537.7 mm and maximum in region VI of 1660.7 mm. The annual sunshine duration varies from 1800 h to 2600 h from south to north, and the relatively humidity increases from 60% in north to 80% in south. The topography of the CAC is dominated by plains at an altitude below 200 m in regions I ~ IV, and hills at an altitude below 500 m in regions V and VI generally.

The CAC is located in the East Asian monsoon region, where north winds prevails in winter and southeast monsoon in summer, resulting in cold and dry climate in most coastal areas in winter while abundant rainfall in summer. The weather is changeable in spring but is generally sunny with little cloud in autumn. Due to the influence of monsoon, seasonal and spatial distributions of precipitation are not uniform and this high precipitation variability makes coastal area a drought- and flood-frequently and consequently a vulnerable region.

2.2. Data

Daily precipitation data of 210 meteorological stations from 1961 to 2014 were available for this study, which are provided by the National Climate Centre, China Meteorological Administration. Quality control such as missing data processing, standard deviation test and abnormal data screening were carried out by RClimDex software. The double-mass curve method (Su et al., 2006), which was often used in the hydrometeorological field to test the homogeneity of precipitation and runoff records was applied to assess the precipitation data series homogeneity for each meteorological station in this study. Finally, 156 meteorological stations with historical records continuous and spanning longer than 50 years were selected.

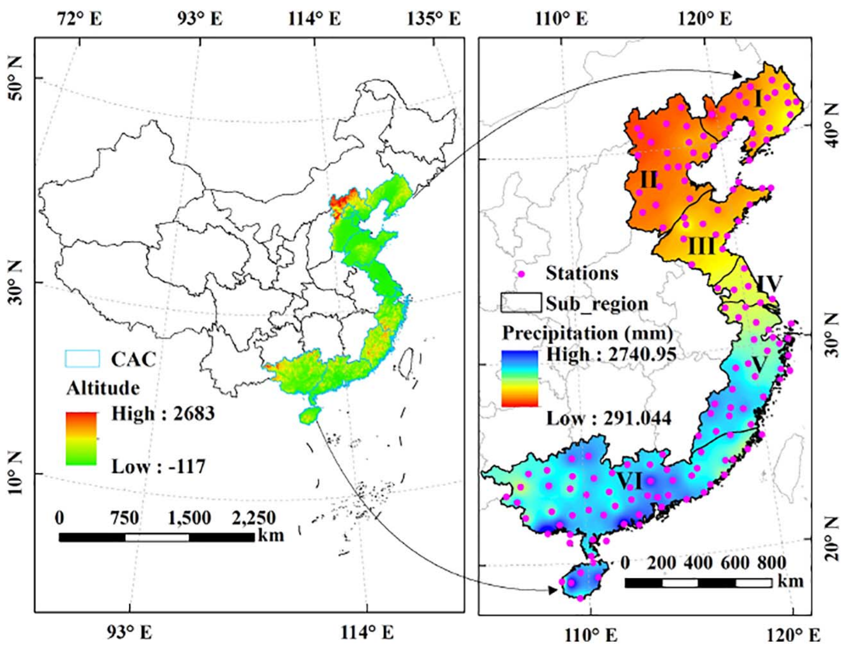

Fig. 1. Location map of the coastal area of China and the meteorological stations.

2.3. Methods

Eleven extreme precipitation indices (Table 1) which have relatively low noise, weak extremes, and strong significance (Frich, 1999) were selected for each meteorological station based on the indicators recommended by the World Meteorological Organization CCL/CLIVAR/JCOMM Expert Team on Climate Change Detection and Indices (ETCCDI). These indices were widely used to evaluate climate change of extreme precipitation events over different regions of the world. According to the definitions, the eleven extreme precipitation indices were classified into two types: indices in precipitation (RX1day, RX5day, R95p, R99p, SDII and PRCPTOT) and indices in the number of precipitation days (R10, R20, R25, CDD and CWD) in this study. All these indices were calculated using the RClimDex software which was developed by researchers from Canadian Meteorological Service (Zhang et al., 2005).

Long-term trend magnitudes in precipitation indices on annual scale were calculated by non-parametric Sen's slop estimator (Sen, 1968). And the trend magnitudes for each meteorological station were expressed into slopes per decade, which were employed to depict the spatial patterns in extreme precipitation indices. The statistical significance for a trend in precipitation index was estimated using the non-parametric Mann-Kendall trend test, and a trend was considered to be statistically significant at the 95% confidence level (Kendall, 1975). Furthermore, Hurst index *H* (formulas given by Hurst (1951)) was estimated by R/S method to test the persistence of tendency for time series in extreme precipitation indices. The Hurst index *H* varies between 0 and 1. A value of 0.5 indicates lack of long-term persistence, and values larger (smaller) than 0.5 mean the presence of long-term persistence (anti-persistence) for series.

The Continuous Wavelet Transform (CWT), which provides an ideal opportunity to localize time and frequency information in studying non-stationary trends was used to detect the periodicity of the extreme precipitation indices series in the current study (Jiang et al., 1997; Torrence and Compo, 1998). What's more, the Morlet wavelet was chosen for the time-frequency analyses because it provides a good balance between time and frequency localization. Detailed information of CWT algorithms and application was introduced in Torrence and Compo (1998). Considering the highly heterogeneity of extreme precipitation in space and time, three mutation test methods including Mann-Kendall mutation test, accumulative anomaly method and Pettitt test which were thoroughly introduced in Wang et al. (2012), Wei (2007) and Pettitt (1979), respectively, were all employed to identify the abrupt change of the time series in extreme precipitation indices.

Moreover, each sub-region was taken as the research subject for period analysis and mutation analysis since the huge complexity and diversity of climate type in the CAC from north to south. Taking indices in precipitation in region VI as examples, the features of wavelet period

Table 1
Definitions of the eleven extreme precipitation indices used in this study.

Index	Descriptive name	Definition	Units
RX1day	Maximum 1-day precipitation amounts	Annual maximum 1-day precipitation	mm
RX5day	Maximum 5-day precipitation amounts	Annual maximum consecutive 5-day precipitation	mm
R95p	Very wet day precipitation	Annual total precipitation when RR > 95th percentile	mm
R99p	Extremely wet day precipitation	Annual total precipitation when RR > 99th percentile	mm
SDII	Simple daily intensity index	Average precipitation on wet days	mm/day
PRCPTOT	Wet-day precipitation	Annual total PRCP in wet days (RR ≥ 1 mm)	mm
R10	Number of heavy precipitation days	Annual count of days when RR ≥ 10 mm	days
R20	Number of very heavy precipitation days	Annual count of days when RR ≥ 20 mm	days
R25	Number of extremely heavy precipitation days	Annual count of days when RR ≥ 25 mm	days
CDD	Consecutive dry days	Maximum number of consecutive dry days	days
CWD	Consecutive wet days	Maximum number of consecutive wet days	days

Abbreviation is as follows: RR, daily precipitation. A wet day is defined when RR ≥ 1 mm and a dry day is when RR < 1 mm. Full definitions of the eleven extreme precipitation indices are available from the ETCCDI website http://etccdi.pacificclimate.org/indices_def.shtml.

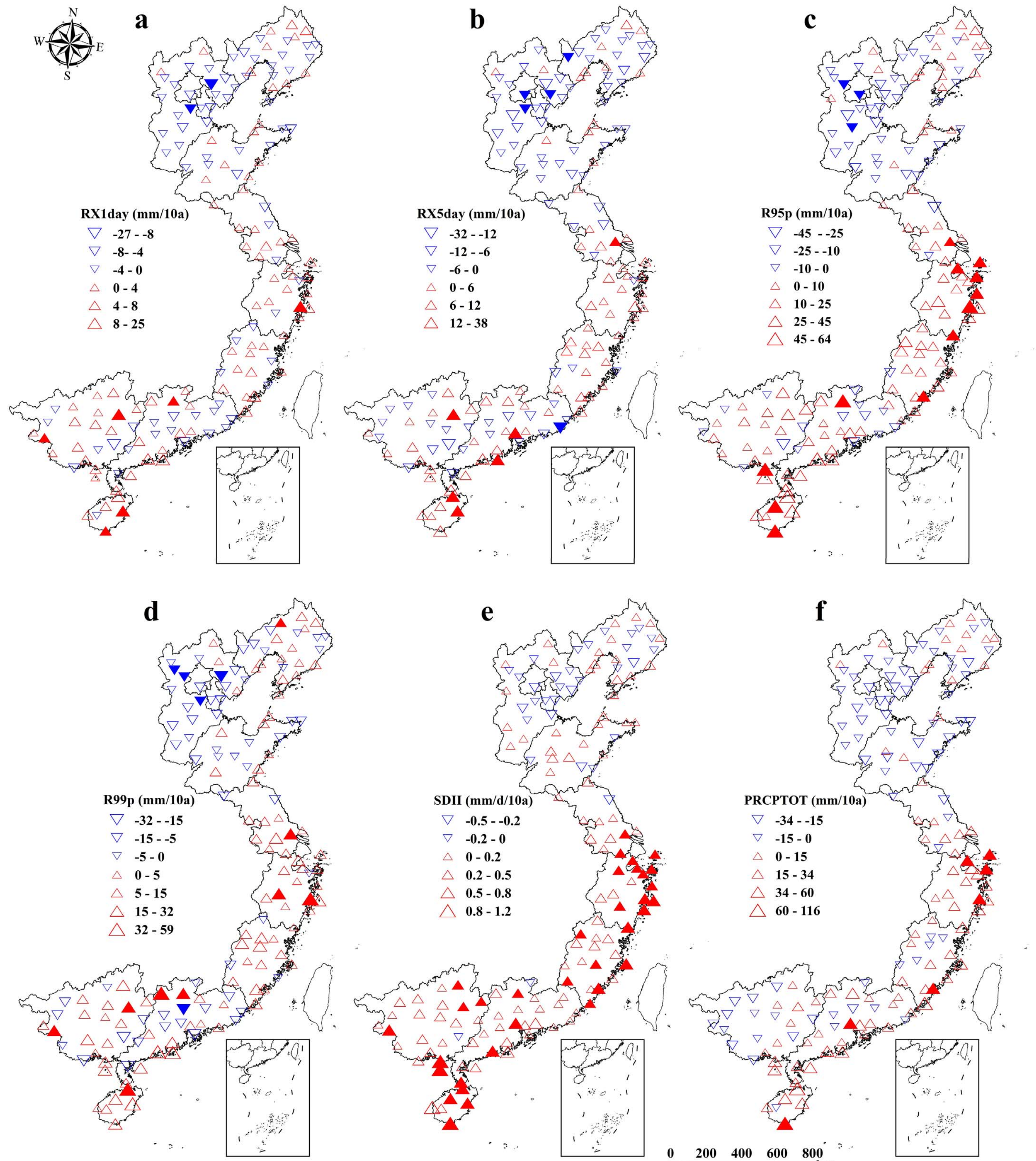

Fig. 2. Spatial distribution of decadal trend rate for **a** RX1day, **b** RX5day, **c** R95p, **d** R99p, **e** SDII, and **f** PRCPTOT over CAC during 1961–2014. Upward and downward triangles indicate positive and negative trends, respectively, and solid triangles represent significant trends at the 95% confidence level while hollow triangles refer to no significance, which are the same as following figures.

and mutation test were analyzed in detail, and results of period analysis and mutation test for time series of extreme precipitation indices in other sub-regions were shown in the corresponding tables only.

3. Results

3.1. Spatial variation of extreme precipitation events

3.1.1. Indices in precipitation

The spatial distribution of decadal trend rate for indices in precipitation over CAC from 1961 to 2014 is shown in Fig. 2. There were approximately 54% and 50% meteorological stations experiencing an increase in RX1day (Fig. 2a) and RX5day (Fig. 2b), respectively, and only both 6 stations out of 156 showed significant positive trends. The stations with upward trends in RX1day and RX5day were both mainly located in the southern coastal areas, and the stations with downward trends were both generally distributed in the northern coastal areas, with 2 and 5 stations which mainly distributed in region II showing significant negative trends for RX1day and RX5day, respectively. R95p (Fig. 2c) and R99p (Fig. 2d) increased for 63% and 60% of the total stations, and there were only 12 and 9 stations with significant upward trends and 3 and 5 stations with significant downward trends for R95p and R99p, respectively. Almost 79% and 53% stations indicated an increase in SDII (Fig. 2e) and PRCPTOT (Fig. 2f), respectively, and about 22% and 4% stations showed significant upward trends, but no station experienced significant downward trend in both SDII and PRCPTOT. In general, the spatial distribution of trends for R95p, R99p, SDII and PRCPTOT were similar to those of RX1day and RX5day, i.e. upward trends in the south and downward trends in the north.

3.1.2. Indices in the number of precipitation days

Fig. 3 demonstrated the spatial patterns for the indices in the number of precipitation days over CAC during 1961–2014. For R10 (Fig. 3a), downward trends occurred at 54% stations which were distributed across the study area, and the 46% stations with upward trends were mainly located in region IV, south of regions V and VI. There were almost 54% and 61% stations with increasing trends in R20 (Fig. 3b) and R25 (Fig. 3c), respectively, which were both distributed mainly in the southern coastal area, and the stations with decreasing trends of R20 and R25 were both mainly located in the northern coastal area. For R10, R20 and R25, there were 3, 10 and 11 stations which were all in the southern coastal area presenting significant positive trends, respectively. Nearly 60% stations increased in CDD (Fig. 3d), mainly in regions I, III and VI, and the other 40% downward stations were mainly located in regions II, VI, and V. Few stations with significant trend scattered across the coastal area in CDD. 69% stations in CWD (Fig. 3e) had downward trend throughout the coastal area, and negative trends of 9% stations which distributed discretely in the CAC was significant.

3.2. Temporal variation of extreme precipitation events

3.2.1. Decade variation of extreme precipitation indices

The multi-year average and decadal trend rate for all extreme precipitation indices over CAC and its six sub-regions from 1961 to 2014 are presented in Table 2.

All extreme precipitation indices except CWD increased from 1961 to 2014 in the entire CAC, among which R95p and SDII showed significant upward trend. The trends of extreme precipitation indices in the entire CAC were different from those in each sub-region, and the multi-year averages and decadal trend rates varied between each sub-region. Specifically,

1) *For indices in precipitation*: The multi-year averages of all indices in precipitation presented a same pattern of "south-high and north-low", with the maximum and minimum in region VI and region II, respectively. RX1day in regions II–IV exhibited declining trends, while RX1day in regions I, V and VI showed upward trends. Except regions V and VI, RX5day in the other sub-regions experienced decreasing trends, and a most pronounced downward trend was found in region II. R95p and R99p presented upward trends in all sub-regions except regions II and III, and the greatest significant positive trend occurred in region V for both R95p and R99p. For SDII, a weak upward trend was found in all sub-regions except region II, and significant upward trends were only found in regions V and VI. PRCPTOT showed downward trends in the northern three sub-regions and upward trends in the southern three sub-regions, however, the trends were insignificant in all sub-regions.
2) *For indices in the number of precipitation days*: Except CDD, the multi-year averages of the other indices in the number of precipitation days presented the same pattern of "south-high and north-low", similar to that of indices in precipitation, and the maximum and minimum for multi-year averages were also found in region VI and region II, respectively. R10, R20 and R25 decreased slightly in the northern three sub-regions but increased in the southern three sub-regions (with significant upward trend in region V for R25 only). CDD was noticed increasing trends in regions I, III and VI and decreasing trends in other sub-regions. All six sub-regions in CWD experienced downward trends which were significant in regions II and III only.

3.2.2. Persistence prediction of tendency in extreme precipitation indices

The Hurst index (Table 3) of tendency in extreme precipitation indices was calculated according to the series of annual averages from 1961 to 2014. In general, random walk and weak persistence and anti-persistence for tendency in extreme precipitation indices were noticed over CAC and its sub-regions. Specifically, with respect to the entire CAC, Hurst index of tendency in R95p, PRCPTOT, CDD, R10, R20 and R25 were all < 0.5, indicating that these extreme indices will showing a tendency opposite to that of the past, and the other extreme indices whose Hurst index of tendency were higher than 0.5 would continue the trends of the past. On sub-region scale, anti-persistence was found for almost all extreme precipitation indices in both regions I and IV except R95p in region I and CDD in region IV, and persistence of trend was detected in RX5day, R99p, R20 and R25 in regions II and III and in SDII, PRCPTOT, R10, R20 and R25 in regions V and VI, respectively, which illustrated that trends of extreme precipitation events in Huabei, Huanghuai, Jiangnan and Huanan coastal areas would continue but trends in Dongbei and Jianghuai coastal areas would mostly present contrary to the past in the future.

3.2.3. Period analysis of extreme precipitation indices

Fig. 4 illustrated the results of wavelet analysis for the time series of indices in precipitation in region VI from 1961 to 2014. The GWS of RX1day and RX5day both experienced significant inter-annual variability (1.8- to 4.2-year periods) with a primary period (major significant period) of 2.3-year, which was both mostly caused by the significant modulations during 1970–1980 and 2005–2010 (Fig. 4a, b). The GWS exhibited a primary period of 6.6-year for R95p, with no corresponding temporal range of significant variation for this cycle in the WPS (Fig. 4c). The GWS and WPS of R99p showed a primary period of 2.3-year, which was due to significant variances in this scale during 2005–2011 (Fig. 4d). A significant 6.6-year period was indentified for SDII, but there was no corresponding temporal range of significant modulation for this cycle in the WPS (Fig. 4e). The GWS of PRCPTOT showed significant inter-annual variability with the periods of 1.8- to 4.7-year, and a 3.9-year peak cycle was found during 1994–2006 in the WPS (Fig. 4f).

The primary periods for extreme precipitation indices in six sub-regions varied from each other (Table 4). In specific,

1) *For indices in precipitation*: The primary period of RX1day was 2.3-year in all sub-regions except region I with a 3.3-year cycle. For

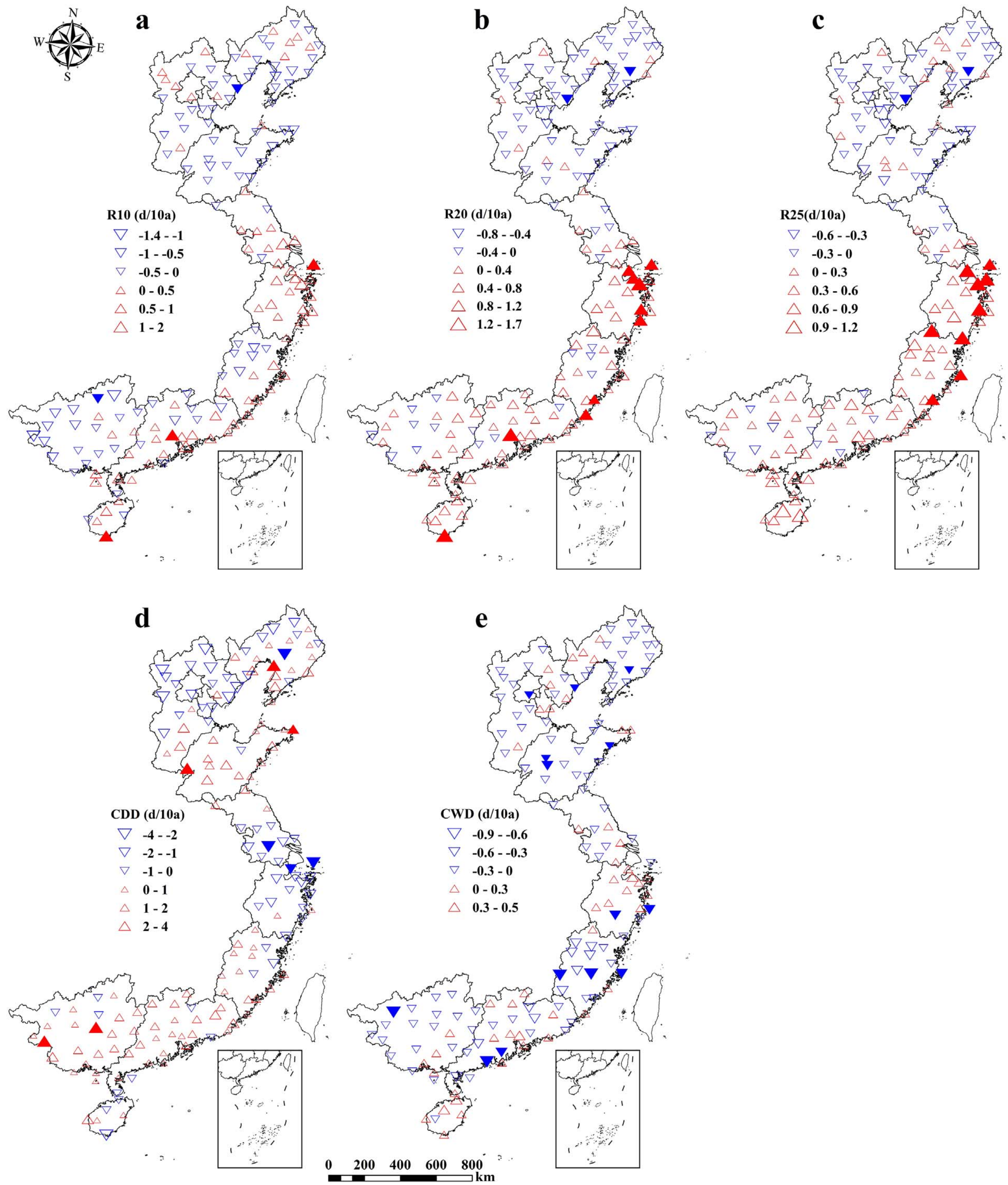

Fig. 3. Spatial distribution of decadal trend rate for **a** R10, **b** R20, **c** R25, **d** CDD, and **e** CWD over CAC during 1961–2014.

RX5day, a longer primary cycle with 5.6-year was identified in region IV while 2- to 4-year cycles were found in other sub-regions. There was generally an increasing trend of primary period for R95p from north to south, with the longest cycle of 6.6-year in region VI. Except 3.9-year in region VI, the other sub-regions all experienced a primary period of 2.3-year for R99p. Comparatively, significant cycles in south sub-regions were much longer than those in north sub-regions for SDII. Regarding to PRCPTOT, in addition to a 5.6-year and 4.7-year primary period in region IV and region III, respectively, the major periods in other sub-regions were 2- to 4-year.

2) *For indices in the number of precipitation days*: 5.6-year primary periods for R10 and R20 and a 4.7-year primary period for R25 were detected in region IV, while primary cycles in other sub-regions was 2- to 5-year for R10, R20 and R25. Regarding to CDD, a longer primary period with 3.3-year was noticed in region I, and 2.8-year cycles were found in other sub-regions. 2- to 4-year primary cycles were discovered for CWD in all sub-regions except region IV with a 5.6-year period.

It is found that significant short period is detected in all sub-regions in the CAC. Possibly due to the temporal range of precipitation data is not long enough, there is no significant inter-decadal cycle observed by

Table 2
Multi-year average and decadal trend rate in the CAC and its sub-regions during 1961–2014.

Index	I		II		III		IV		V		VI		CAC	
	Ma	Rat	Ma	Rat	Ma	Rat	Ma	Rat	Ma	Rat	Ma	Rat	Ma	Rat
RX1day	83.81	0.32	72.95	**−2.90**	96.55	−0.92	99.01	−0.40	99.43	1.64	136.79	**2.62**	107.06	0.78
RX5day	126.98	−0.80	110.05	**−5.27**	144.61	−1.65	159.34	−0.62	177.64	**4.19**	234.41	3.84	177.62	1.08
R95p	190.60	1.49	147.99	**−9.83**	218.24	−2.27	290.74	5.28	372.84	**22.31**	479.34	16.29	334.04	**8.89**
R99p	62.27	1.49	47.92	**−6.79**	71.12	−0.70	95.96	6.22	122.76	**9.45**	159.07	7.20	110.21	3.76
SDII	11.70	0.02	11.03	−0.10	13.06	0.11	12.82	0.09	12.67	**0.31**	15.69	**0.35**	13.47	**0.19**
PRCPTOT	666.10	−5.43	530.73	−13.66	739.37	−14.98	1020.62	7.52	1429.54	24.18	1644.63	14.03	1178.47	5.63
R10	19.08	−0.17	15.24	−0.16	20.25	−0.47	29.80	0.33	43.89	0.34	43.60	0.11	32.88	0.02
R20	9.43	−0.16	7.32	−0.18	10.67	−0.20	14.61	0.01	21.46	0.56	24.65	0.34	17.42	0.16
R25	6.98	−0.10	5.42	−0.19	8.22	−0.19	10.75	0.07	15.59	**0.54**	19.29	0.31	13.28	0.16
CDD	60.04	0.29	74.88	−0.61	48.77	1.23	32.98	−0.55	29.05	−0.63	38.48	0.81	46.44	0.24
CWD	4.35	−0.09	4.01	**−0.08**	4.44	**−0.13**	5.63	−0.04	8.06	−0.09	8.69	−0.09	6.69	−0.09

Abbreviations are as follows: Ma, multi-year average. Rat, decadal trend rate. Characters in bold referred to trend significant at 95% confidence level.

Table 3
Hurst index of tendency in extreme precipitation indices in the CAC.

Index	I	II	III	IV	V	VI	CAC
RX1day	0.45	0.47	0.49	0.49	0.60	0.44	0.57
RX5day	0.48	0.55	0.51	0.43	0.47	0.46	0.51
R95p	0.50	0.49	0.54	0.44	0.47	0.38	0.47
R99p	0.47	0.52	0.51	0.42	0.54	0.49	0.59
SDII	0.49	0.49	0.55	0.47	0.54	0.51	0.55
PRCPTOT	0.47	0.48	0.54	0.42	0.53	0.56	0.43
CDD	0.41	0.42	0.48	0.55	0.34	0.46	0.38
CWD	0.41	0.48	0.63	0.43	0.44	0.56	0.57
R10	0.49	0.51	0.49	0.37	0.54	0.61	0.47
R20	0.44	0.52	0.53	0.37	0.56	0.59	0.48
R25	0.49	0.51	0.55	0.45	0.55	0.57	0.46

CWT in this study.

3.2.4. Mutation analysis of extreme precipitation indices

Fig. 5 revealed the Mann-Kendall mutation test (*left panel*) and cumulative anomaly variations (*right panel*) for the time series of indices in precipitation in region VI during 1961–2014. In each subplot on left panel, the two curves of Mann-Kendall *U* values for the forward and backward statistical sequences are represented by UF and UB, respectively. For RX1day, UF and UB statistic curves had an intersection within the confidence interval between 1997 and 1998 (Fig. 5a, *left panel*). And the cumulative anomaly of RX1day decreased before 1992 but increased after then (Fig. 5a, *right panel*). What's more, Pettitt test indicated that time series of RX1day mutated in 1992. Thus RX1day in region VI experienced a “less to more” mutation around 1992. Mann-Kendall test and cumulative anomaly variations for the time series of RX5day, R95p, R99p, SDII and PRCPTOT in region VI in Fig. 5b, c, d, e and f, respectively, revealed that these extreme precipitation indices mutated from less to more around 1992.

Table 5 gives the mutation time and tendency for the time series of extreme precipitation indices in six sub-regions of the CAC. To be specific,

1) *For indices in precipitation*: With respect to RX1day and RX5day, a mutation was noticed mainly in the latest 1970s in regions II and III while mostly in the 1990s in other sub-regions. Besides region III, mutation times for both R95p and R99p in other sub-regions occurred in the 1980s or the early 1990s. For SDII, all sub-regions experienced a sudden change in the 1980s or the early 1990s except region II. The abrupt change for PRCPTOT in regions III, IV and V appeared in the 1970s or the 1980s, but in the 1990s for other three sub-regions.
2) *For indices in the number of precipitation days*: For R10, mutations were found in the 1970s in all sub-regions except regions II and IV, what's more, both R20 and R25 suffered from an abrupt change in the same time as R10 in the corresponding sub-region generally. The mutation time which distributed in the 1970s to the 1990s varied across sub-regions for CDD. Except regions I–III, CWD in other sub-regions all experienced an abrupt change in the early 21st.

Fig. 6 demonstrated the number of extreme precipitation indices which suffered from mutation in the sub-regions in each decade. Among all extreme precipitation indices in all sub-regions, there were 24, 21 and 15 indices getting mutations in the 1990s, the 1970s and the 1980s, respectively, and there were both only 3 indices showing abrupt changes in the 1960s and in the early 21st, respectively, which revealed that extreme precipitation events mutated mainly in the 1990s and the 1970s, followed by the 1980s. Based on the tendency in extreme precipitation indices before and after mutation (Table 5), it was clear that with exception of CWD, which was noticed a mutation from more to less in all sub-regions, most extreme precipitation indices experienced an abrupt change of “less to more” in regions I, IV, V and VI while a mutation of “more to less” in regions II and III. It is further known that extreme precipitation events in regions I, IV, V and VI with abundant rainfall had mutated into a higher incidence period while in regions II and III with limited rainfall had changed into a lower incidence stage.

4. Discussion and conclusion

Many earlier studies found that extreme precipitation events showed an increasing trend around the world (Alexander et al., 2006; Griffiths and Bradley, 2007; You et al., 2011; Madsen et al., 2014; Naidu et al., 2015). In this study, an upward trend was detected for extreme precipitation indices such as PRCPTOT, R95p, R99p, SDII, RX1day, RX5day, and so on, in the CAC during 1961–2014, which were consistent with the results of earlier studies. Regional difference was also found about the trend in extreme precipitation indices over CAC. For example, sub-regions located in the semi-humid area, such as coastal areas of Huabei and Huanghuai, were prone to be suffered from a decreasing trend of precipitation extremes, similar to the previous studies over China (You et al., 2011), the northern China (Zhao et al., 2013), the Circum-Bohai-Sea region in the north of China (Jiang et al., 2011) and the Loess Plateau (Sun et al., 2016). In contrast, sub-regions in the southern coastal areas with abundant rainfall had a rising trend of precipitation extremes, which agreed with the results of You et al. (2011), Du et al. (2013) and Zhao et al. (2014). The trends of extreme precipitation events over CAC demonstrated that reduced precipitation extremes would exacerbated drought pressure and regional water shortages in the northern coastal areas, but flood disasters had been aggravated due to the ascending trend of extreme precipitation events in the southern coastal areas during 1961–2014. It should be noted that precipitation extremes would generally continue to drop in the semi-

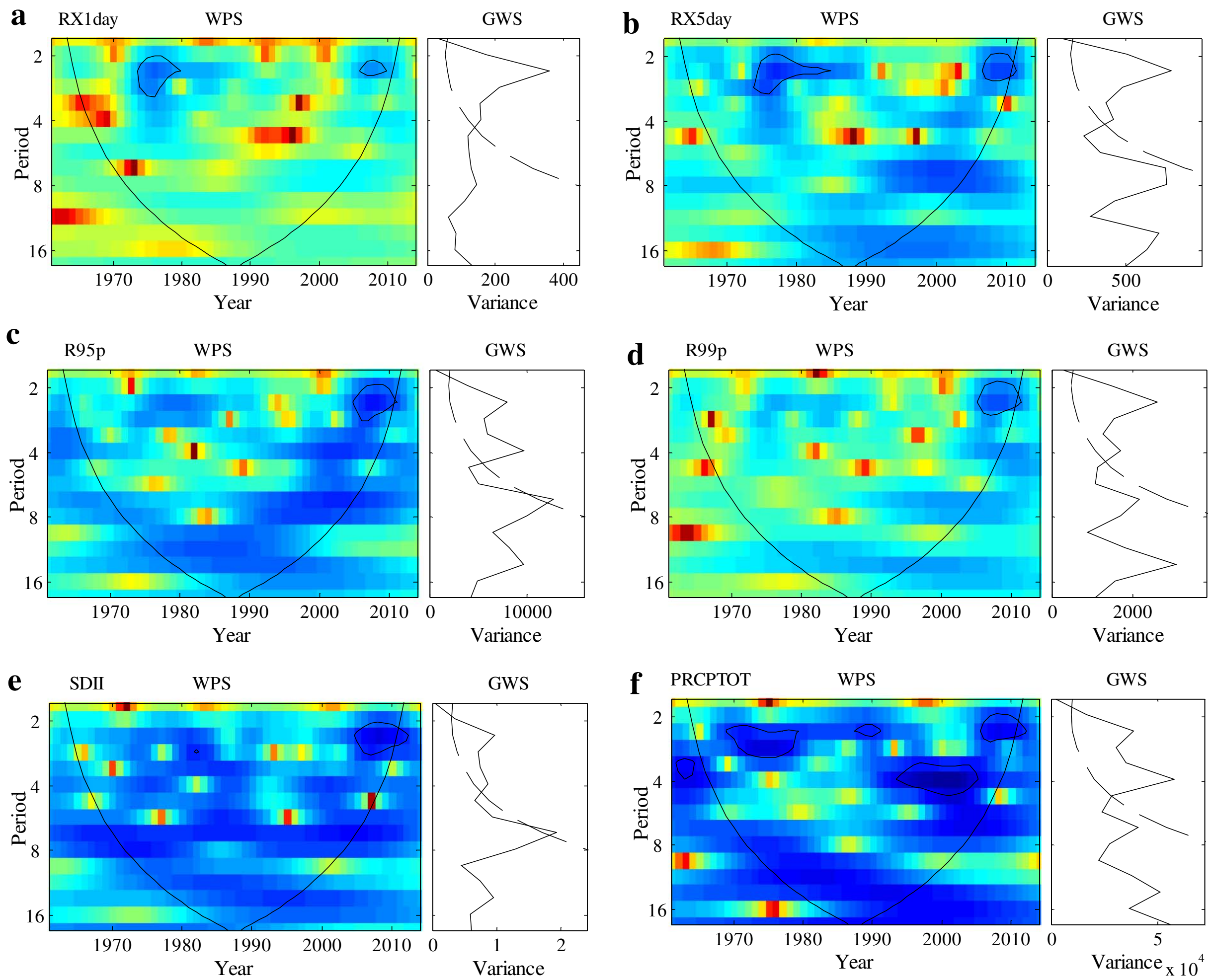

Fig. 4. The Wavelet Power Spectrum (WPS) and the Global Wavelet Spectrum (GWS) for the time series of **a** RX1day, **b** RX5day, **c** R95p, **d** R99p, **e** SDII, and **f** PRCPTOT in region VI. The black closed contours of WPS and the dashed curve of GWS designated the significance level $\alpha = 95\%$ against red noised, and the cone of influence (COI) where edge effects might distort was shown as the U-shaped curve.

Table 4
Primary period (year) of extreme precipitation indices in the sub-regions.

Index	I	II	III	IV	V	VI
RX1day	3.3	2.3	2.3	2.3	2.3	2.3
RX5day	3.3	3.3	3.3	5.6	3.9	2.3
R95p	2.8	2.3	2.3	5.6	3.9	6.6
R99p	2.3	2.3	2.3	2.3	3.9	2.3
SDII	3.3	3.9	2.3	5.6	3.3	6.6
PRCPTOT	2.3	2.8	4.7	5.6	3.9	3.9
R10	2.3	2.8	2.8	5.6	3.9	3.9
R20	2.8	2.8	4.7	5.6	3.9	3.9
R25	2.8	2.8	4.7	2.3	3.9	3.9
CDD	3.3	2.8	2.8	2.8	2.8	2.8
CWD	2.8	3.9	3.9	5.6	3.9	2.3

humid coastal areas in the north but would rise persistently in the humid coastal areas in the south according to the results of Hurst index, which would further intensify the situation of “south-flood and north-drought” over CAC in the coming period.

A major change of extreme precipitation events in the 1970s and the 1990s over CAC was found in this study, and a similar result was also detected in previous studies in China (Hu et al., 2003; Yao et al., 2008), the eastern China (Ding et al., 2008) and the southern China (Wu et al., 2010). Researchers carried out plenty studies on influencing factors of precipitation variation during past several decades, and found that El Niño-Southern Oscillation (ENSO), Tibetan Plateau snow, atmospheric circulation and sea surface temperature (SST), and so on all played important roles in rainfall variability in China. For example, notable changes in atmospheric circulation had been observed over East Asia and its neighboring western Pacifica around the late 1970s (Wu and Wang, 2002), significant weakening of the East Asian summer monsoon (Ding et al., 2008), and changes in SSTs in the tropical Pacific and Indian Ocean (Wu et al., 2010), which were all likely to be responsible for the abrupt change of precipitation and its extremes in China. What's more, it is found that precipitation over the Yangtze River region tended to be above normal when the warm ENSO mature phase forms in the summer (Lau and Weng, 2001; Wu et al., 2003), and the changes of Tibetan Plateau snow had an impact on the rainfall variability in eastern and whole China (Zhao et al., 2007; Wang et al., 2008). Especially worth noting that as a transitional zone between the ocean and inland, the CAC is totally under the influence of various large-scale climate factors such as monsoon, atmospheric circulation, ocean currents, and so on, which all would affect the precipitation and its extremes more profoundly.

Furthermore, the primary period and mutation time of extreme precipitation indices varied across the sub-regions, which can be not only attributed to the reasons mentioned above but also the differences of natural geographical along the coast and influences of anthropogenic activities (Jiao et al., 2015). For example, topography and landform, land cover, hydrological conditions, soil type and other natural geographical factors, and anthropogenic activities such as emission of greenhouse gas, Urban Heat Island (UHI), sea reclamation, artificial

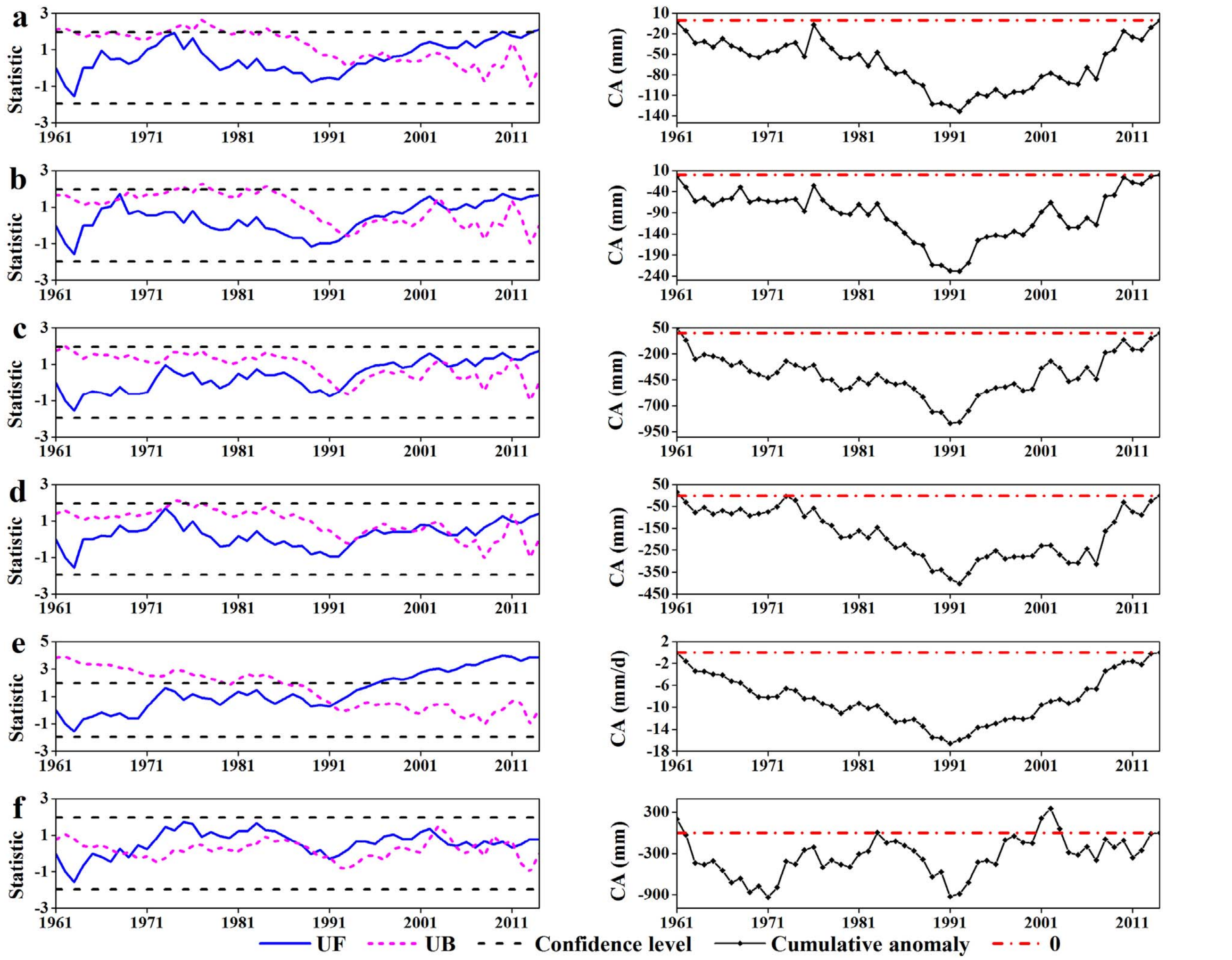

Fig. 5. Mann-Kendall test (*left panel*) and cumulative anomaly curves (*right panel*) for the time series of **a** RX1day, **b** RX5day, **c** R95p, **d** R99p, **e** SDII, and **f** PRCPTOT in region VI. Abbreviation CA referred to Cumulative Anomaly.

afforestation and deforestation and so on, which all had remarkable impacts on precipitation variability in the CAC. In addition, the differentiations of extreme precipitation events among the sub-regions are intensified furtherly both by the spatial heterogeneity in precipitation (Tammets and Jaagus, 2012) and suddenness in its extremes (Sura, 2011) in the CAC.

Variation of extreme precipitation events in the coastal area of China have been investigated based on daily precipitation dataset of 156 meteorological stations during 1961–2014. Results showed that except a downward trend was found in CWD in the sub-regions as well as the entire coastal area, the other extreme precipitation indices generally presented decreasing trends in regions I, II and III while increasing trends in regions IV, V and VI. Persistent of tendency revealed that trends of extreme precipitation events in regions II, III, V and VI would be the same as in the past but would present contrary to the past in regions I and IV in the coming period. With respect to regionally

Table 5
Mutation time (year) and tendency of extreme precipitation indices series in six sub-regions over CAC during 1961–2014.

Index	I		II		III		IV		V		VI	
	MT	TE	MT	TE	MT	TE	MT	TE	MT	TE	MT	TE
RX1day	1993–1994	↑	1979–1980	↓	1965	↓	1972	↓	1988	↑	1992	↑
RX5day	1998	↓	1979–1980	↓	1978	↓	1993	↓	1991–1992	↑	1992–1993	↑
R95p	1993–1994	↑	1979	↓	1965	↓	1983	↑	1986	↑	1991–1992	↑
R99p	1993–1994	↑	1988	↓	1965	↓	1984	↑	1988	↑	1992	↑
SDII	1993–1994	↑	1979	↓	1993	↑	1982	↑	1986	↑	1991–1992	↑
PRCPTOT	1996	↓	1996	↓	1975	↓	1983–1984	↑	1986–1987	↑	1991–1992	↑
R10	1977	↓	1996	↓	1975	↓	1981–1982	↑	1972	↑	1971	↑
R20	1977	↓	1996	↓	1975	↓	1979	↑	1986	↑	1971	↑
R25	1998	↓	1996	↓	1975	↓	1978	↑	1986–1987	↑	1971	↑
CDD	1987	↑	1977–1978	↓	1993	↑	1981	↓	1995	↓	1975	↑
CWD	1990–1991	↓	1996	↓	1978	↓	2011	↓	2002	↓	2002	↓

Abbreviations are as follows: MT, mutation time. TE, tendency. Symbols of "↑" and "↓" indicate extreme precipitation event experienced mutation of "less to more" and "more to less", respectively.

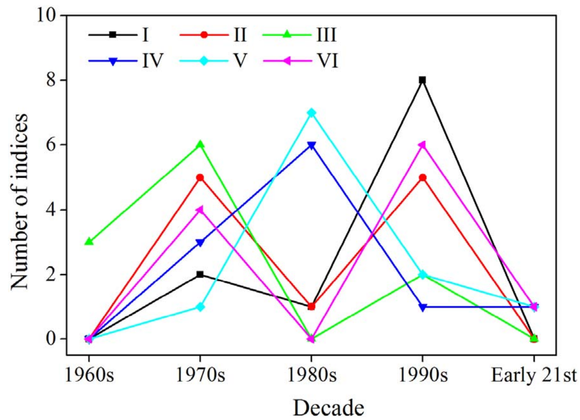

Fig. 6. Number of extreme precipitation indices which suffered mutation in the sub-regions in each decade.

multi-year averages, except for CDD declining from north to south generally, a similar distribution with "south-high and north-low" in other extreme precipitation indices was identified, and the maximum and minimum for multi-year averages were found in region VI and region II, respectively. For sub-regions, the primary period of extreme precipitation indices ranged from 2- to 7-year, but inter-decadal period was not significant. Additionally, the abrupt change of extreme precipitation indices occurred mainly in the 1990s and the 1970s in the CAC.

Acknowledgments

This research was financially supported by the National Natural Science Foundation of China (Belmont Forum Collaborative Research Action on Scenarios of Biodiversity and Ecosystem Services, NSFC-BF/IGFA, No. 31461143032). The authors kindly thank the National Climate Centre (NCC) of China Meteorological Administration (CMA) for providing the data in this study. Wavelet software was provided by C. Torrence and G. Compo, and is available at http://paos.colorado.edu/research/wavelets/. The constructive comments and suggestions of the reviewers are gratefully acknowledged.

References

Alexander, L.V., Zhang, X.B., Peterson, T.C., Caesar, J., Gleason, B., Klein Tank, A., Haylock, M., Collins, D., Trewin, B., Rahimzadeh, F., 2006. Global observed changes in daily climate extremes of temperature and precipitation. J. Geophys. Res. Atmos. 111, D05109.
Boccolari, M., Malmusi, S., 2013. Changes in temperature and precipitation extremes observed in Modena. Italy. Atmos. Res. 122, 16–31.
Cavalcanti, I.F.A., 2012. Large scale and synoptic features associated with extreme precipitation over South America: a review and case studies for the first decade of the 21st century. Atmos. Res. 118, 27–40.
Cavalcanti, I.F.A., Carril, A.F., Penalba, O.C., Grimm, A.M., Menéndez, C.G., Sanchez, E., Cherchi, A., Sörensson, A., Robledo, F., Rivera, J., 2015. Precipitation extremes over La Plata Basin – review and new results from observations and climate simulations. J. Hydrol. 523, 211–230.
Chen, F., Chen, H., Yang, Y., 2015. Annual and seasonal changes in means and extreme events of precipitation and their connection to elevation over Yunnan Province. China. Quatern. Int. 374, 46–61.
Cinco, T.A., de Guzman, R.G., Hilario, F.D., Wilson, D.M., 2014. Long-term trends and extremes in observed daily precipitation and near surface air temperature in the Philippines for the period 1951–2010. Atmos. Res. 145-146, 12–26.
Croitoru, Adina-Eliza, Chiotoroiu, Brîndușa-Cristina, Ivanova Todorova, V., Torică, V., 2013. Changes in precipitation extremes on the Black Sea western coast. Glob. Planet. Chang. 102, 10–19.
Deng, H., Chen, Y., Shi, X., Li, W., Wang, H., Zhang, S., Fang, G., 2014. Dynamics of temperature and precipitation extremes and their spatial variation in the arid region of northwest China. Atmos. Res. 138, 346–355.
Ding, W., 2014. Spatial and temporal variability of the extreme daily precipitation in southwest China. Resour. Environ. Yangtze basin. 23 (7), 1071–1079 (in Chinese).
Ding, Y., Wang, Z., Sun, Y., 2008. Inter-decadal variation of the summer precipitation in East China and its association with decreasing Asian summer monsoon. Part I: Observed evidences. Int. J. Climatol. 28, 1139–1162.
Dong, S., Tao, S., Yang, W., Li, F., Li, S., Li, Y., Liu, H., 2010. Impacts of climate change on urban agglomerations in coastal region of China. Adv. Clim. Chang. Res. 6 (4), 284–289 (in Chinese).
Du, Y.D., Ai, H., Duan, H.L., Hu, Y.M., Wang, X.W., He, J., Wu, H.Y., Wu, X.X., 2013. Changes in climate factors and extreme climate events in South China during 1961–2010. Adv. Clim. Chang. Res. 4 (1), 1–11.
Frich, P., 1999. REWARD: A Nordic Collaborative Project. Annex of Meeting of the Joint CCl/CLIVAR Task Group on Climate Indices, Bracknell, UK, 2–4 September 1998// Folland, C.K., Horton, E.B., Scholefield, P.R., World Climate Data and Monitoring Programme, WCDMP-No.37, WMO-TD No.930. World Meteorological Organization, Geneva.
Griffiths, M.L., Bradley, R.S., 2007. Variations of twentieth-century temperature and precipitation extreme indicators in the Northeast United States. J. Clim. 20 (21), 5401–5417.
Hu, Z.Z., Yang, S., Wu, R.G., 2003. Long-term climate variations in China and global warming signals. J. Geophys. Res. Atmos. 108 (D19), ACL11.1–ACL11.13.
Hurst, H.E., 1951. Long-term storage capacity of reservoirs. Trans. Am. Soc. Civ. Eng. 116, 770–779.
Jena, P.P., Chatterjee, C., Pradhan, G., Mishra, A., 2014. Are recent frequent high floods in Mahanadi basin in eastern India due to increase in extreme rainfalls? J. Hydrol. 517, 847–862.
Jiang, J., Zhang, D., Fraedrich, K., 1997. Historic climate variability f wetness in East China (960–1992): a wavelet analysis. Int. J. Climatol. 17, 969–981.
Jiang, D., Wang, K., Li, Z., Wang, Q., 2011. Variability of extreme summer precipitation over Circum-Bohai-Sea region during 1961–2008. Theor. Appl. Climatol. 104, 501–509.
Jiang, C., Shaw, K.S., Upperman, C.R., Blythe, D., Mitchell, C., Murtugudde, R., Sapkota, A.R., Sapkota, A., 2015. Climate change, extreme events and increased risk of salmonellosis in Maryland, USA: evidence for coastal vulnerability. Environ. Int. 83, 58–62.
Jiao, N.Z., Chen, D.K., Luo, Y.M., Huang, X.P., Zhang, R., Zhang, H.B., Jiang, Z.J., Zhang, F., 2015. Climate change and anthropogenic impacts on marine ecosystems and countermeasures in China. Adv. Clim. Chang. Res. 6 (2), 118–125.
Keggenhoff, I., Elizbarashvili, M., Amiri-Farahani, A., King, L., 2014. Trends in daily temperature and precipitation extremes over Georgia, 1971–2010. Weather Clim. Extremes. 4, 75–85.
Kendall, M.R., 1975. Multivariate Analysis. Charles Griffin, London.
Knapp, A.K., Beier, C., Briske, D.D., Classen, A.T., Luo, Y., Reichstein, M., Smith, M.D., Smith, S.D., Bell, J.E., Fay, P.A., 2008. Consequences of more extreme precipitation regimes for terrestrial ecosystems. Bioscience 58 (9), 811–921.
Lau, K.M., Weng, H., 2001. Coherent models of global SST and summer rainfall over China: an assessment of the regional impacts of the 1997–98 El Niño. J. Clim. 14, 1294–1308.
Li, Z., Liu, W.Z., Zhang, X.C., Zheng, F.L., 2011. Assessing the site-specific impacts of climate change on hydrology, soil erosion and crop yields in the Loess Plateau of China. Clim. Chang. 105, 223–242.
Ly, M., Traore, S.B., Alhassane, A., Sarr, B., 2013. Evolution of some observed climate extremes in the West African Sahel. Weather Clim. Extremes. 1, 19–25.
Madsen, H., Lawrence, D., Lang, M., Martinkova, M., Kjeldsen, T.R., 2014. Review of trend analysis and climate change projections of extreme precipitation and floods in Europe. J. Hydrol. 519, 3634–3650.
Naidu, C.V., Dharma Raju, A., Satyanarayana, G.C., Vinay Kumar, P., Chiranjeevi, G., Suchitra, P., 2015. An observational evidence of decrease in Indian summer monsoon rainfall in the recent three decades of global warming era. Glob. Planet. Chang. 127, 91–102.
Nie, C., Li, H., Yang, L., Ye, B., Dai, E., Wu, S., Liu, Y., Liao, Y., 2012. Spatial and temporal changes in extreme temperature and extreme precipitation in Guangxi. Quat. Int. 263, 162–171.
Päädam, K., Post, P., 2011. Temporal variability of precipitation extremes in Estonia 1961–2008. Oceanologia 53 (1-TI), 245–257.
Pettitt, A.N., 1979. A non-parametric approach to the change-point problem. Appl. Stat. 28, 126–135.
Powell, J.P., Reinhard, S., 2016. Measuring the effects of extreme weather events on yields. Weather Clim. Extremes. 12, 69–79.
Ren, Z., Zhang, M., Wang, S., Zhu, X., Dong, L., Qiang, F., 2014. Changes in precipitation extremes in South China during 1961–2011. Acta. Geograph. Dermatol. Sin. 69 (5), 640–649 (in Chinese).
Rimkus, E., Kažys, J., Bukantis, A., Krotovas, A., 2011. Temporal variation of extreme precipitation events in Lithuania. Oceanologia 53, 259–277.
Sen, P.K., 1968. Estimates of the regression coefficient based on Kendall's tau. J. Am. Stat. Assoc. 63 (324), 1379–1389.
Song, X., Song, S., Sun, W., Mu, X., Wang, S., Li, J., Li, Y., 2015. Recent changes in extreme precipitation and drought over the Songhua River Basin, China, during 1960–2013. Atmos. Res. 157, 137–152.
Su, B.D., Jiang, T., Jin, W.B., 2006. Recent trends in observed temperature and precipitation extremes in the Yangtze River basin, China. Theor. Appl. Climatol. 83, 139–151.
Subash, N., Singh, S.S., Priya, Neha, 2011. Extreme rainfall indices and its impact on rice productivity—a case study over sub-humid climatic environment. Agr. Water. Manage. 98 (9), 1373–1387.
Sun, W., Mu, X., Song, X., Wu, D., Cheng, A., Qiu, B., 2016. Changes in extreme temperature and precipitation events in the Loess Plateau (China) during 1960-2013 under global warming. Atmos. Res. 168, 33–48.
Sura, P., 2011. A general perspective of extreme events in weather and climate. Atmos. Res. 101, 1–21.
Tammets, T., Jaagus, J., 2012. Climatology of precipitation extremes in Estonia using the method of moving precipitation totals. Theor. Appl. Climatol. 111, 623–639.

Torrence, C., Compo, G.P., 1998. A practical guide to wavelet analysis. Bull. Amer. Meteor. Soc. 79, 61–78.
Tramblay, Y., Badi, W., Driouech, F., El Adlouni, S., Neppel, L., Servat, E., 2012. Climate change impacts on extreme precipitation in Morocco. Glob. Planet. Chang. 82-83, 104–114.
Wang, B., Bao, Q., Hoskins, B., Wu, G., Liu, Y., 2008. Tibetan Plateau warming and precipitation changes in East Asia. Geophys. Res. Lett. 35, L14702.
Wang, H., Zhang, M., Zhu, H., Dang, X., Yang, Z., Yin, L., 2012. Hydro-climatic trends in the last 50 years in the lower reach of the Shiyang River Basin, NW China. Catena 95, 33–41.
Wang, S., Zhang, M., Wang, B., Sun, M., Li, X., 2013. Recent changes in daily extremes of temperature and precipitation over the western Tibetan Plateau, 1973–2011. Quat. Int. 313-314, 110–117.
Wang, M., Yan, J., Li, S., 2014. Spatial-temporal variation and the tendency of droughts and floods on the southeast coast of China over 54 years. Resour. Sci. 36 (11), 2307–2315 (in Chinese).
Wei, F., 2007. Modern climate statistics diagnosis and prediction technology. China Meteorological Press. 1–256 (in Chinese).
Wen, G., Huang, G., Tao, W., Liu, C., 2015. Observed trends in light precipitation events over global land during 1961–2010. Theor. Appl. Climatol. 125, 161–173.
Willems, P., 2013. Adjustment of extreme rainfall statistics accounting for multidecadal climate oscillations. J. Hydrol. 490, 126–133.
Wu, R., Wang, B., 2002. A contrast of the East Asian summer monsoon-ENSO relationship between 1962-77 and 1978-93. J. Clim. 15, 3266–3279.
Wu, R., Hu, Z., Kirtman, B.P., 2003. Evolution of ENSO-related rainfall anomalies in East Asia. J. Clim. 16, 3742–3758.
Wu, R., Wen, Z., Yang, S., Li, Y., 2010. An interdecadal change in southern China summer rainfall around 1992/93. J. Clim. 23 (9), 2389–2403.
Xu, X., Du, Y., Tang, J., Wang, Y., 2011. Variations of temperature and precipitation extremes in recent two decades over China. Atmos. Res. 101, 143–154.
Yao, C., Yang, S., Qian, W., Lin, Z., Wen, M., 2008. Regional summer precipitation events in Asia and their changes in the past decades. J. Geophys. Res. 113, D17107.
Yi, F., Zhang, X., Hu, K., 2011. A review of researches on land-ocean interaction in the coastal zone. Mar. Geol. Front. 27 (3), 28–34 (in Chinese).
You, Q., Kang, S., Aguilar, E., Pepin, N., Flügel, Wolfgang-Albert, Yan, Y., Xu, Y., Zhang, Y., Huang, J., 2011. Changes in daily climate extremes in China and their connection to the large scale atmospheric circulation during 1961–2003. Clim. Dyn. 36, 2399–2417.
Zhang, X., Hegerl, G., Zwiers, F.W., Kenyon, J., 2005. Avoiding inhomogeneity in percentile-based indices of temperature extremes. J. Clim. 18, 1641–1651.
Zhang, Q., Xu, C.Y., Chen, Y.D., Yang, T., 2009. Spatial assessment of hydrologic alteration across the Pearl River Delta, China, and possible underlying causes. Hydrol. Process. 23 (11), 1565–1574.
Zhang, Q., Li, J., Chen, X., Bai, Y., 2011. Spatial variability of probability distribution of extreme precipitation in Xinjiang. Acta Geograph. Sin. 66 (1), 3–12 (in Chinese).
Zhao, P., Zhou, Z., Liu, J., 2007. Variability of Tibetan spring snow and its associations with the hemispheric extratropical circulation and East Asian summer monsoon rainfall: an observational investigation. J. Clim. 20, 3942–3955.
Zhao, C.Y., Wang, Y., Zhou, X.Y., Cui, Y., Liu, Y.L., Shi, D.M., 2013. Changes in climatic factors and extreme climate events in Northeast China during 1961–2010. Adv. Clim. Chang. Res. 4 (2), 92–102.
Zhao, Y., Zou, X., Cao, L., Xu, X., 2014. Changes in precipitation extremes over the Pearl River Basin, southern China, during 1960–2015. Quat. Int. 333, 26–39.